Proc. of SPIE Vol. 1998, Optomechanical Design, ed. D Vukobratovich, P R Yoder, V L Genberg (Sep 1993) Copyright SPIE

Design of a cell for the wide-field corrector for the converted MMT

Robert Fata and Daniel Fabricant

Harvard-Smithsonian Center for Astrophysics
60 Garden Street, Cambridge, Massachusetts 02138

ABSTRACT

We describe an approach for mounting the ~0.8 m diameter optical elements in a refractive corrector for the Multiple Mirror Telescope (MMT). The optical elements are mounted on discrete pads of RTV rubber to an Invar/carbon steel cell. Following the conversion of the MMT to use a single 6.5 m primary mirror, the corrector will provide up to a 1° diameter field-of-view for multi-object spectroscopy with optical fibers or for wide-field imaging.

1. INTRODUCTION

The Multiple Mirror Telescope (MMT), which is jointly operated by the Smithsonian Institution and the University of Arizona, will be converted to use a single 6.5 m primary mirror in 1995. One of the major incentives for this conversion is to increase the field of view of the MMT from its current 3′ diameter. Harland Epps has designed a three element refractive corrector (with all fused silica elements) that produces excellent images over a curved 1° diameter field at the f/5.4 focus of the converted telescope. A pair of counter-rotating zero-deviation prisms provide atmospheric dispersion compensation (ADC). (Each of the ADC prisms contains elements of UV-transmitting FK5 and LLF6 glass bonded together.) The initial application of this focus will be multi-object spectroscopy with optical fibers. The corrector can be reconfigured by removing one of the lenses and the ADC prisms and adding a different fused silica lens. In this alternate configuration the corrector provides a flat 0.5° diameter field for imaging. In both configurations the corrector is designed for the spectral band 0.33–1.1 μm.

In this paper we describe our mounting concept for the corrector elements, which are typically 0.8 m in diameter. The corrector cell must support the elements with minimal distortion under varying gravitational loads and over a wide temperature range (-15 °C to 25 °C). The corrector cell must allow periodic removal of the corrector elements to renew the antireflection coatings because the best available broad-band antireflection coatings are easily damaged. The space available for the corrector cell is limited because the corrector elements are mounted in the Cassegrain hole of the primary mirror.

To satisfy these requirements we have designed a cell with both Invar and carbon steel components. The coefficient of thermal expansion (CTE) mismatches between the cell materials and the optical elements are compensated by using elastomer (RTV rubber) pads for radial support. The elements are located in the axial direction by machined steps in the cell and additional elastomer pads. The performance of the mounting concept has been evaluated with finite element models and with ray traces of the deformed optical surfaces.

2. CELL DESIGN

The cell consists of a main assembly that houses the two lead fused silica elements and two interchangeable subassemblies that are used for either spectroscopy or imaging. Those portions of

the cell that house fused silica elements are machined from Invar 39 (with a CTE of 2.3×10^{-6} °C^{-1}); the mounting flange and those portions of the cell housing the ADC prisms are made from carbon steel (with a CTE of 12×10^{-6} °C^{-1}). The two configurations are shown in Fig. 1 and 2. Flexures at the interface between the Invar and carbon steel portions of the cell accommodate the CTE mismatch.

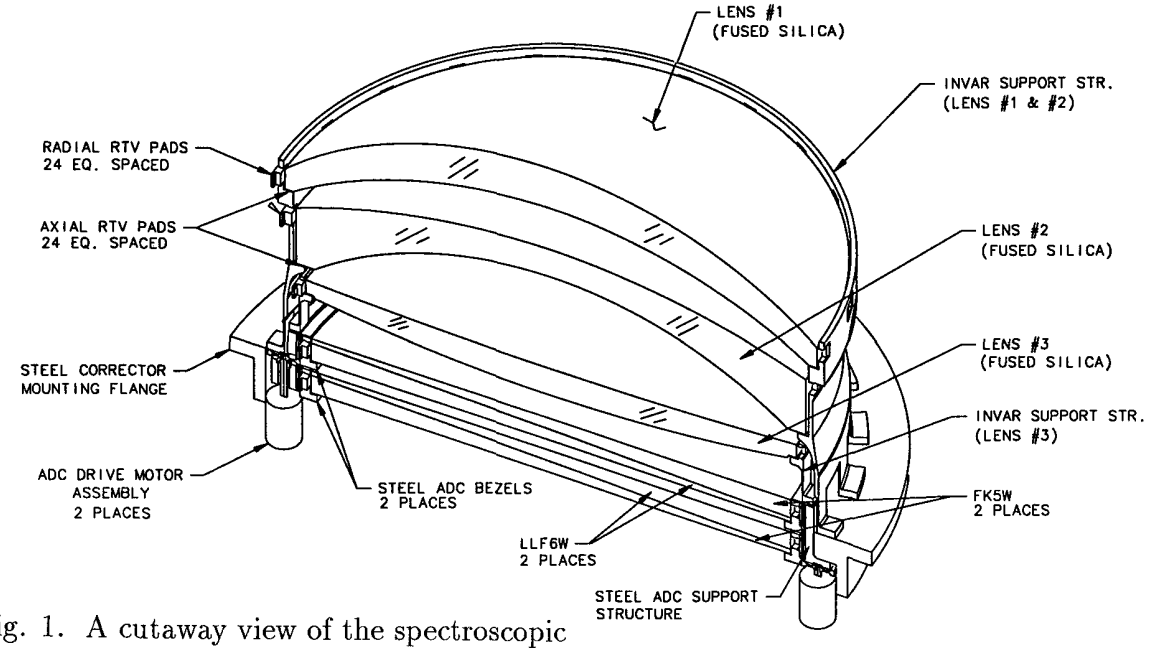

Fig. 1. A cutaway view of the spectroscopic corrector configuration.

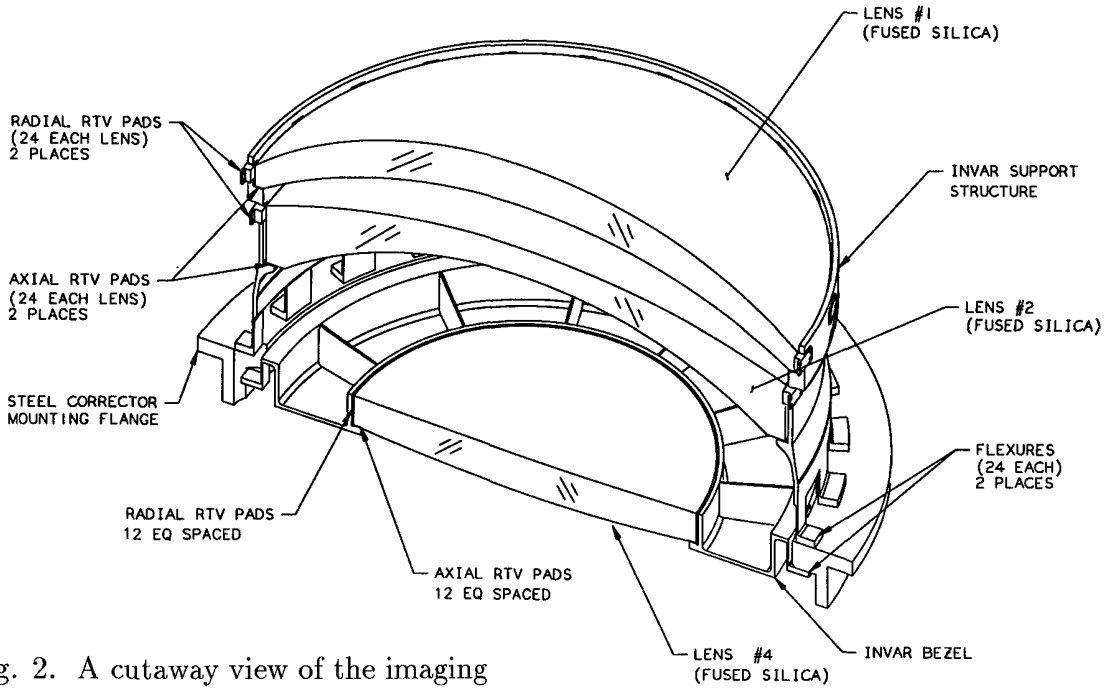

Fig. 2. A cutaway view of the imaging corrector configuration.

The optical elements in the corrector have diameters ranging from 0.50–0.84 m. These elements cannot be supported adequately by a machined steel surface, since in practice this would result in a three point mount. Our analysis shows that a minimum of 12 axial supports are required. (In practice we sometimes use 24 pads to obtain the desired stiffness and pad geometry.) Our approach is to use compliant, precast RTV pads that will partially absorb the machining irregularities on the mounting surface. Our studies have indicated that if the combined irregularities of the cell and the axial RTV pads are held to ~25 μm, the resulting distortion of the optical elements will be less than 0.25 μm, which will not degrade the optical performance of the corrector. The precast axial pads will be bonded to the cell with a thin layer of RTV and tested for uniform height. The assembly will begin with lowering an optical element onto the axial pads and centering the element with respect to the cell. The centration tolerances of ~75 μm can be achieved by reference to machined surfaces. After each element is aligned in the cell, radial RTV pads are installed at the locations of the axial pads around its circumference. The radial pads will be bonded to individual mounting brackets to ease their installation. Fig. 3 is an exploded view of the RTV pad mounting arrangement.

Fig. 3. An exploded view of the RTV pad mounting arrangement.

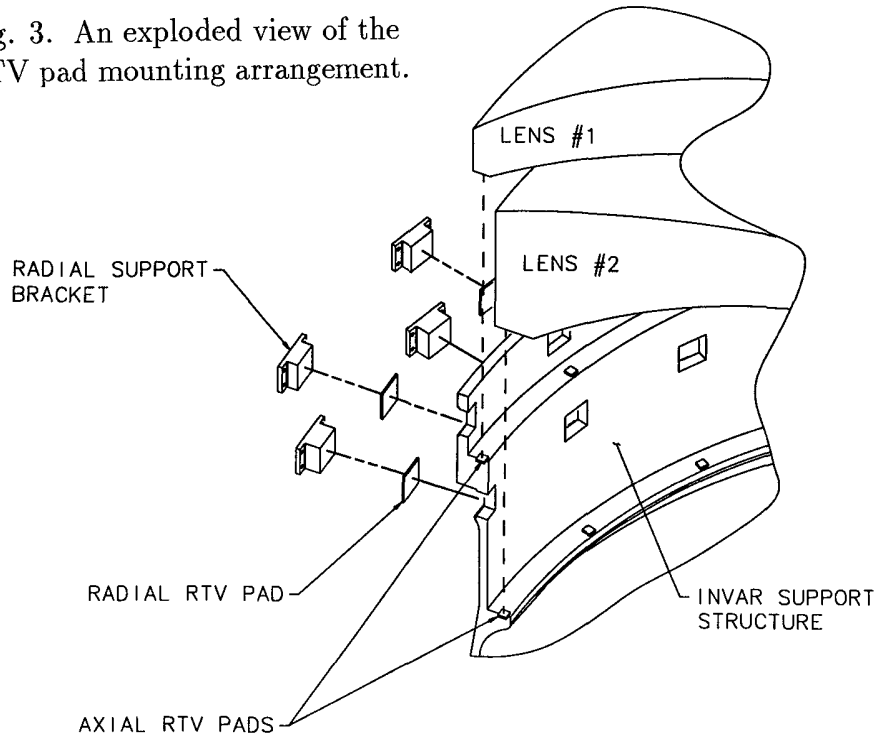

3. SIZING THE RTV PADS

We chose RTV560 (manufactured by GE Silicones) for its high strength (4.8 $\times 10^6$ N m^{-2} in tension), tolerance of a wide temperature range (-115 °C to 260 °C), low shrinkage (1.0%), and a viscosity that is suitable for precision casting. (For those struggling with the metric system, 1×10^6 N m^{-2} corresponds to 145 psi.) The Shore A durometer hardness of RTV560 is 55 according to the manufacturer. Assuming that RTV behaves like natural rubber (and that Shore A and IRHD scales are equivalent), we can derive some important mechanical properties from the durometer specification:[1]

E_o (Young's modulus)	3.3×10^6 N m^{-2}
G (Shear modulus)	0.81×10^6 N m^{-2}
E_* (Bulk modulus)	1090×10^6 N m^{-2}
k (material factor)	0.64

Measurements of E_o and G as a function of temperature are available.[2] At 25 °C, the measured value for G is 0.82×10^6 N m^{-2} and for E_o is 3.5×10^6 N m^{-2}. These are in excellent agreement with the values derived from the durometer specification. Furthermore, these values vary by less than 15% from –60 °C to 90 °C.[2]

A major consideration in the design of the RTV pads is the effect of their shape factor (S) on their mechanical properties. The shape factor is defined as the ratio of the loaded area (single face) divided by the force free area (see Fig. 4). The geometry of the pad is important because the bulk modulus (E_*) of RTV (or natural rubber) is much larger than the Young's modulus (E_o). This means that the pads will deform under load without changing their total volume significantly. The incompressibility of the pads prevents them from deforming under load if space is not available for them to bulge. The shape factor of the pads affects their stiffness (or compression modulus, Ec) and their CTE in the direction perpendicular to the plane of the loaded surfaces of the pad. The shear stiffness of the pads does not depend strongly on their geometry.

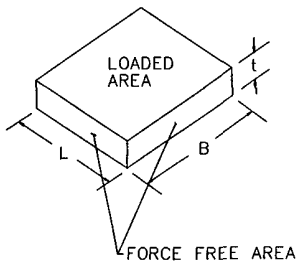

Fig. 4. The definition of the shape factor.

The compression modulus for circular or rectangular blocks is derived using the following formula:[1]

$$E_c = E_o(1 + 2kS^2)$$

The effective CTE of the RTV, α_{RTV}, is given by:

$$\alpha_{RTV} = \alpha_0 K_T$$

where α_0 is the nominal CTE and K_T is a correction factor that depends on the shape factor.[3] K_T for a shape factor of 4.0 (appropriate for our radial pads) is 2.75, α_0 for RTV560 is 198×10^{-6} °C^{-1}. This correction factor has been verified experimentally for RTV11.[4] RTV11 has a Shore A durometer of 41, but the thermal correction factor is only weakly dependent on the hardness of the material.

The corrections for shape factor are important; if they were neglected, the compression modulus and the CTE for the radial RTV pads would be in error by factors of 21 and 2.7, respectively.

3.1. Axial RTV Pads

The thickness of the axial RTV pads is chosen so that their deflection under the load of the optical elements is 10% of the total pad thickness. The load-deflection curve for RTV in compression is non-linear; however, this non-linearity can be ignored for strains up to 10%. Our objective is to allow enough compliance to absorb irregularities on the mounting surface without distorting the optical elements.

We chose a shape factor of 1.0 for the axial pads, which gives $E_c = 7.4 \times 10^6$ N m^{-2}. A square pad (with S=1.0) has a thickness to width ratio of 0.25. The axial RTV pads are typically 6.4 mm wide and 1.6 mm thick.

3.2. Radial RTV Pads

The radial pads are ideally placed at the axial center-of-gravity of the optical element, but due to the large curvature of the fused silica lenses this is not always possible. We chose a shape factor of 4.0 for the the radial pads, which gives $E_c = 70 \times 10^6$ N m^{-2}. The radial pads supply additional axial support and most of the translational stiffness. The thickness of the radial pads is determined from the following equation, which is easily derived from geometrical considerations:

$$t = \frac{R(\alpha_{cell} - \alpha_{lens})}{\alpha_{RTV} - \alpha_{cell}}$$

where R is the lens radius, and the various α's refer to the material CTE's. Satisfying this equation athermalizes the structure and lens so that stresses or deformations caused by a uniform temperature change are theoretically eliminated. We intend to measure the CTE's of each material and adjust the RTV thickness accordingly. With a shape factor of 4.0, a square pad has a thickness to width ratio of 0.0625. The radial pads are typically 21 mm wide and 1.3 mm thick.

To approximately match the stiffness of each optical element mount, 24 axial pads and 24 radial pads are used for the two heavier fused silica lenses. The remaining lenses and the ADC prism assemblies use 12 axial pads and 12 radial pads. This match is desirable to minimize the relative displacements of the optical elements due to gravity. A match to 20% in stiffness was achieved. The fundamental frequencies and mode shapes for each optical element on its RTV pads are: a ~55 Hz axial translation mode, a ~70 Hz tip/tilt mode, a ~70 Hz rotational mode (about the optical axis), and a ~300 Hz lateral translation mode.

4. FINITE ELEMENT MODEL

All finite element analysis including pre- and post-processing was carried out with the I-DEAS software published by the Structural Dynamics Research Corporation. Half symmetry models have been used throughout, with the appropriate boundary conditions applied along the line of symmetry. Solid elements are used to accurately model the varying thicknesses and large curvatures of the lenses. Beam elements are used to represent the axial and radial RTV pads. The beam elements incorporate the compression modulus (E_c) and the CTE calculated using the appropriate shape factor.

Thin shell elements are used to model the support structures with the exception that beam elements are used to represent the axial mounting flanges and that solid elements are used to represent the steel mounting flange (due to its non-uniform cross-sectional area and relatively large depth). Fig. 5 shows the finite element model for the spectroscopy configuration.

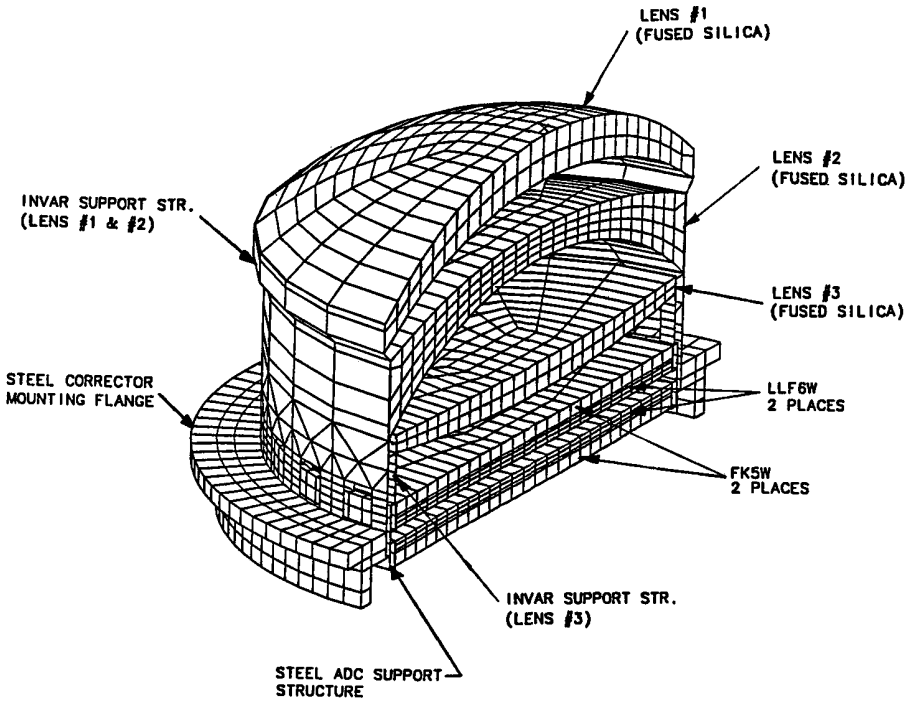

Fig. 5. The finite element model of the spectroscopy configuration.

5. STRESS ANALYSIS

We calculated the maximum stress levels resulting from the combination of gravity and temperature changes for each of the structural components and optical elements used in the spectroscopic configuration. (The corrector is tilted with respect to the Earth's gravitational field as the MMT is pointed at various elevations.) The temperature effects were calculated assuming that the assembly is isothermal, but that the CTE's of the various materials are only known to 10% accuracy (the CTE errors were combined in the least favorable combination). We adopt a conservative maximum temperature swing of 40 °C.

The maximum allowable stress in the optical elements is taken to be 3.4 $\times 10^6$ N m^{-2} (500 psi). The maximum allowable stress in the Invar components is taken to be the microyield stress of 124 $\times 10^6$ N m^{-2} to ensure repeatable behavior following thermal cycling of the flexures. The maximum allowable stress in the steel components is taken to be the yield stress of 207 $\times 10^6$ N m^{-2}.

The maximum stress levels (from the finite element model) computed for the optical elements is 2.3 $\times 10^6$ N m^{-2}. The maximum stress level computed for the structure is 110 $\times 10^6$ N m^{-2} in the Invar flexures. The major contributor to these maximum stress levels is the assumed CTE mismatch with a 40 °C temperature change.

The stress levels in the RTV are low. The maximum stress in the axial RTV pads is a compressive stress of 0.7 $\times 10^6$ N m^{-2} due to gravity. The maximum stress in the radial RTV pads is 1.2 $\times 10^6$ N m^{-2} resulting from the 40 °C temperature change. All of the shear stress levels in the RTV pads are below 0.1 $\times 10^6$ N m^{-2}.

6. RAY TRACING THE FINITE ELEMENT RESULTS

In order to determine the optical effect of the gravitational and thermal loads discussed in Sections 4 and 5, the deformed surfaces of the optical elements predicted by the finite element model were fit with Zernike polynomials. Zernike polynominals of low order (5th order spherical aberration was the highest order used) fit the deformed surfaces to an accuracy of 0.02 μm or better. Zernike fits to deformed surfaces can be ray-traced by several optical design programs; we used ZEMAX EE, which is published by Focusoft, Inc. We examined monochromatic and polychromatic spot diagrams for three situations: with the corrector zenith pointing, with the corrector horizon pointing, and with a temperature change of 40 °C (CTE's uncertain to 10%).

The effects of gravity appear to be completely negligible, and the thermal distortions appear to be quite small as well. The most severe thermally induced effect observed with the spectroscopic configuration is the degradation of the monochromatic RMS image diameter on-axis from 0.06″ to 0.14″ (at 0.46 μm). The degradation is less pronounced for polychromatic images off-axis because it is obscured by a small amount of lateral color.

7. CONCLUSION

The performance of the the corrector cell meets our goals, at least on paper. We are currently carrying out the detailed mechanical design of the cell. We intend to refine our RTV pad casting skills to produce pads with a thickness tolerance of $\sim$10 μm. We also intend to measure the CTE's of the materials used in the corrector, because large CTE errors may produce unacceptable stresses and noticeable image degradation. The other material properties are apparently well enough understood for our purposes, although it may be prudent to test the uniformity of the compression modulus of the RTV pads.

8. REFERENCES

1. P. B. Lindley, "Engineering Design with Natural Rubber", *Natural Rubber Technical Bulletin*, 3rd edition, published by the National Rubber Producers Research Association, 1970.

2. T. Bergeron, "Potting Test on RTV560 and PR1578", *Itek Interoffice Memorandum*, October 17, 1984.

3. R. H. Finney, "Springy Finite Elements Model Elastomer", *Machine Design*, Vol. 58, No. 12, pp. 87-92, May, 1986.

4. A. J. Lobdell, "Effect of Shear Restraint on the Properties of RTV-11", *Itek Interoffice Memorandum*, November 13, 1968.